Mon. Not. R. Astron. Soc. **000**, 1–?? (2008)   Printed 20 August 2008   (MN LaTeX style file v2.2)

arXiv:0802.0078v2 [astro-ph] 20 Aug 2008

Uniformly Rotating Homogeneous Rings in Newtonian Gravity

Stefan Horatschek* and David Petroff*
Theoretisch-Physikalisches Institut, University of Jena, Max-Wien-Platz 1, 07743 Jena, Germany

20 August 2008

ABSTRACT

In this paper, we describe an analytical method for treating uniformly rotating homogeneous rings without a central body in Newtonian gravity. We employ series expansions about the thin ring limit and use the fact that in this limit the cross-section of the ring tends to a circle. The coefficients can in principle be determined up to an arbitrary order. Results are presented here to the 20th order and compared with numerical results.

Key words: gravitation – methods: analytical – hydrodynamics – stars: rotation.

1 INTRODUCTION

The problem of the self-gravitating ring captured the interest of such renowned scientists as Kowalewsky (1885), Poincaré (1885) and Dyson (1892, 1893). Each of them tackled the problem of an axially symmetric, homogeneous ring in equilibrium by expanding it about the thin ring limit. In particular, Dyson provided a solution to fourth order in the parameter $\sigma = a/b$, where a provides a measure for the radius of the cross-section of the ring and b the distance of the cross-section's centre of mass from the axis of rotation.

First numerical results were given by Wong (1974), who was not able to clarify the transition to spheroidal bodies. Eriguchi & Sugimoto (1981) and Eriguchi & Hachisu (1985) developed improved methods with which they were able to study this transition and the connection to the Maclaurin spheroids. Returning to the problem significantly later, Ansorg, Kleinwächter & Meinel (2003c) achieved near-machine accuracy, which allowed them to study bifurcation sequences in detail and correct erroneous results.

In this paper we provide a scheme to extend Dyson's work up to arbitrary order in σ. With the help of computer algebra[1], we were able to compute the solution explicitly up to the 20th order and see a marked improvement over the fourth order. Although constant mass density is of considerable importance to the method presented here, an extension of it to other equations of state is possible (Petroff & Horatschek 2008).

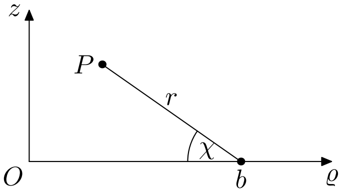

Figure 1. A sketch providing the meaning of the coordinates (r, χ) in relation to the cylindrical coordinates (ϱ, z).

2 THE APPROXIMATION SCHEME

2.1 The Coordinates

To describe axially symmetric rings, we introduce the polar-like coordinates (r, χ, φ), which are related to the cylindrical coordinates (ϱ, z, φ) by

$$\varrho = b - r\cos\chi, \quad z = r\sin\chi, \quad \varphi = \varphi, \tag{1}$$

see also Fig. 1. The surface of the ring will be described by a function $r_s(\chi)$. In our coordinates, the Laplace operator applied to a function $f = f(r, \chi)$ reads

$$\begin{aligned}\nabla^2 f =& \frac{\partial^2 f}{\partial r^2} + \frac{1}{r}\frac{\partial f}{\partial r} + \frac{1}{r^2}\frac{\partial^2 f}{\partial \chi^2}\\ &- (b - r\cos\chi)^{-1}\left(\cos\chi\frac{\partial f}{\partial r} - \frac{\sin\chi}{r}\frac{\partial f}{\partial \chi}\right).\end{aligned} \tag{2}$$

We choose the constant b in such a manner, that the centre of mass of the ring's cross-section coincide with $r = 0$, thus implying

$$\int_0^{2\pi}\int_0^{r_s(\chi)} \mu r^2 \cos\chi \, \mathrm{d}r \, \mathrm{d}\chi = 0, \tag{3}$$

where μ is the mass density.

---

* E-mail: `S.Horatschek@tpi.uni-jena.de` (SH); `D.Petroff@tpi.uni-jena.de` (DP)

[1] We made use of Maple$^{\mathrm{TM}}$. Maple is a trademark of Waterloo Maple Inc.

2.2 Basic Equations

For solving the problem of a self-gravitating fluid in equilibrium, we have to fulfil Laplace's equation

$$\nabla^2 U = 0 \tag{4}$$

outside the fluid and Poisson's equation

$$\nabla^2 U = 4\pi G\mu \tag{5}$$

inside it, where U is the gravitational potential. Additionally, we have to satisfy Euler's equation

$$\mu \frac{\mathrm{d}\boldsymbol{v}}{\mathrm{d}t} = -\mu\nabla U - \nabla p, \tag{6}$$

where $\boldsymbol{v}$ is the velocity of a fluid element and p the pressure. We consider uniform rotation about the axis $\varrho = 0$ with the angular velocity $\boldsymbol{\Omega}$ and thus have the velocity field

$$\boldsymbol{v} = \boldsymbol{\Omega} \times \boldsymbol{x} \tag{7}$$

leading to

$$\nabla\left(U + \int_0^p \frac{\mathrm{d}p'}{\mu(p')} - \frac{1}{2}\Omega^2\varrho^2\right) = 0. \tag{8}$$

Integration gives

$$U + \int_0^p \frac{\mathrm{d}p'}{\mu(p')} - \frac{1}{2}\Omega^2\varrho^2 = V_0, \tag{9}$$

where V_0 is the constant of integration. At the surface of the ring, where the pressure vanishes, we have

$$U_\mathrm{s} - \frac{1}{2}\Omega^2\varrho^2\bigg|_\mathrm{s} = V_0. \tag{10}$$

We are dealing here with homogeneous rings, i.e. the mass density is a constant

$$\mu = \text{constant}. \tag{11}$$

This means that the integral in (8) and (9) is simply p/μ and (3) reduces to

$$\int_0^{2\pi} r_\mathrm{s}(\chi)^3 \cos\chi \,\mathrm{d}\chi = 0. \tag{12}$$

2.3 The Idea of the Approximation Scheme

The thin ring limit is approached when the ratio of the inner radius ϱ_i to the outer one ϱ_o tends to 1. In this limit, the cross-section of the ring becomes a circle. This is the starting point of the approximation. As an interesting aside, if one considers a ring surrounding a central body, for example a point mass, the cross-section of the ring can deviate significantly from a circle even if the radius ratio is close to 1, see Fig. 8 in Ansorg & Petroff (2005).

We describe the surface of the ring by the Fourier series

$$r_\mathrm{s}(\chi) = a\left(1 + \sum_{i=1}^{q}\sum_{k=1}^{i}\beta_{ik}\cos(k\chi)\sigma^i + o(\sigma^q)\right), \tag{13}$$

where

$$\sigma := \frac{a}{b}. \tag{14}$$

There are no sine terms because of reflectional symmetry with respect to the equatorial plane, which is known to hold for fluids in equilibrium (see Lichtenstein 1933). To the leading order, the cross-section is indeed a circle of radius a. We make a similar ansatz for the square of the angular velocity Ω

$$\Omega^2 = \pi G\mu\left(\sum_{i=0}^{q+2}\Omega_i\sigma^i + o(\sigma^{q+2})\right) \tag{15}$$

and V_0

$$V_0 = -\pi G\mu a^2\left(\sum_{i=0}^{q} v_i\sigma^i + o(\sigma^q)\right). \tag{16}$$

Because we consider constant mass density, a given surface function $r_\mathrm{s}(\chi)$ determines the distribution of the mass completely, i.e. one can compute the potential everywhere. For technical reasons, we first calculate the potential on the axis of symmetry only. After this, we determine the potential outside the ring and in particular along its surface, where (10) must hold.

Since the potential outside the ring contains logarithmic terms in r it will come as no surprise that there are $\ln\sigma$ terms in the coefficients of our series. Like Dyson, we introduce

$$\lambda := \ln\frac{8}{\sigma} - 2. \tag{17}$$

Let us suppose that we already know the solution up to the $(q-1)$st order, and want to find the qth order, in particular β_{qk} $(k = 1, 2, \ldots, q)$ and Ω_{q+1}. To find these $q+1$ unknowns, we have to fulfil equation (12) and also require that the q Fourier coefficients in front of $\cos(k\chi)$ $(k = 1, 2, \ldots, q)$ in (10) vanish. After finding these $q+1$ unknowns, we now know v_{q-1}, but cannot yet determine the coefficient v_q.

2.4 The Potential Outside the Ring

First off, the Poisson integral is used to find the value of the potential along the axis of rotation. We label the coordinates for a point on the axis $(R, \chi_R) \equiv (r, \chi)$, from which

$$b = R\cos(\chi_R) \tag{18}$$

follows. The axis potential is

$$\begin{aligned} U_\mathrm{axis}(R) &= -2\pi G \int_0^{2\pi}\int_0^{r_\mathrm{s}(\chi')} \frac{\mu\,(b - r\cos\chi')r}{\sqrt{R^2 + r^2 - 2Rr\cos\psi}}\,\mathrm{d}r\,\mathrm{d}\chi' \\ &= -2\pi G\mu \int_0^{2\pi}\int_0^{r_\mathrm{s}(\chi')} (b - r\cos\chi')\sum_{l=0}^{\infty}\left(\frac{r}{R}\right)^{l+1} P_l(\cos\psi)\,\mathrm{d}r\,\mathrm{d}\chi' \\ &=: -2\pi^2 G\mu a\sum_{l=1}^{\infty}(a^2\sigma^{-1})^l\frac{(2l-1)!!}{2l-1}\frac{A_l}{R^{2l-1}} \end{aligned} \tag{19}$$

where $\psi := \chi' - \chi_R$. Please note that the expansion in terms of powers of $1/R$ indicated in the last line is not trivial, since there is an R-dependence hidden in the terms with ψ. Because of reflectional symmetry, there are only terms with odd powers in $1/R$. We expand A_l with respect to σ

$$A_l = \sum_{i=l-1}^{q}\alpha_{li}\sigma^i + o(\sigma^q). \tag{20}$$

Using U_{axis}, we can then find the potential anywhere in the vacuum region. To do so, we first introduce a set of axially symmetric solutions to Laplace's equation that vanish at infinity. We define

$$I_1(\varrho, z) := \int\limits_0^\pi \frac{\mathrm{d}\varphi}{\sqrt{b^2 + \varrho^2 + z^2 - 2b\varrho\cos\varphi}}, \tag{21}$$

which is nothing other than a multiple of the potential of a circular line of mass with radius b, centred around the axis. In (r, χ, φ)-coordinates it reads

$$I_1(r, \chi) = \frac{2K\left(\sqrt{\frac{4b^2 - 4br\cos\chi}{4b^2 - 4br\cos\chi + r^2}}\right)}{\sqrt{4b^2 - 4br\cos\chi + r^2}}, \tag{22}$$

where K denotes the complete elliptic integral of the first kind,

$$K(k) := \int\limits_0^{\frac{\pi}{2}} \frac{\mathrm{d}\theta}{\sqrt{1 - k^2\sin^2\theta}}. \tag{23}$$

Because the difference of two of such solutions with different b's also satisfies Laplace's equation, it is clear that

$$I_l(r, \chi) := \left(-\frac{1}{b}\frac{\mathrm{d}}{\mathrm{d}b}\right)^{l-1} I_1(r, \chi), \tag{24}$$

where

$$\frac{\mathrm{d}}{\mathrm{d}b} = \frac{\partial}{\partial b} + \cos\chi\frac{\partial}{\partial r} - \frac{\sin\chi}{r}\frac{\partial}{\partial\chi} \tag{25}$$

is also a solution of Laplace's equation. Next we note that along the axis we have

$$I_l(R) = \frac{\pi(2l-1)!!}{(2l-1)R^{2l-1}}. \tag{26}$$

It then follows that the potential in the vacuum region is

$$U_{\mathrm{out}}(r, \chi) = -2\pi G\mu a^2 \left(\sum_{l=1}^{q+1} a^{2l-1}\sigma^{-l} A_l I_l(r, \chi) + o(\sigma^q)\right), \tag{27}$$

since this expression satisfies Laplace's equation, vanishes at infinity and has the correct value along the axis. For calculating the potential at the body's surface we expand $I_l(r, \chi)$ for $r < b$. For example we get

$$I_1(r, \chi) = \frac{1}{b}\left[\ln\left(\frac{8b}{r}\right) + \frac{[\ln(8b/r) - 1]\cos\chi}{2}\frac{r}{b} + o\left(\frac{r}{b}\right)\right]. \tag{28}$$

After evaluating these equations for $I_l(r, \chi)$ at the surface $r = r_{\mathrm{s}}(\chi)$, we use (27) to find the coefficients ϕ_{ik} in the expansion

$$U_{\mathrm{s}}(\chi) = -2\pi G\mu a^2 \left(\sum_{i=0}^{q}\sum_{k=0}^{i} \phi_{ik}\cos(k\chi)\sigma^i + o(\sigma^q)\right). \tag{29}$$

2.5 The Potential Inside the Ring and the Pressure

To treat the interior of the ring, it is convenient to introduce the dimensionless coordinate

$$y := \frac{r}{a}. \tag{30}$$

For calculating the potential inside the ring, we first expand it,

$$U_{\mathrm{in}}(r, \chi) = -\pi G\mu a^2 \sum_{i=0}^{q}\sum_{k=0}^{i} U_{ik}(y)\cos(k\chi)\sigma^i. \tag{31}$$

Inserting this into Poisson's equation (5) and collecting the coefficients in front of $\cos(k\chi)\sigma^i$ gives ordinary differential equations (ODEs) in y for the $U_{ik}(y)$. The solutions to these equations are determined uniquely by requiring that $U_{ik}(y)$ be finite at the centre $y = 0$ and that the potential be continuous at the surface, i.e. $U_{\mathrm{in}}(r_{\mathrm{s}}(\chi), \chi)$ must agree with $U_{\mathrm{s}}(\chi)$.

After solving the ODEs for $U_{ik}(y)$, we know the inner potential, and with (9) we are able to calculate the pressure

$$p(r, \chi) = \pi G\mu^2 a^2 \left(\sum_{i=0}^{q}\sum_{k=0}^{i} p_{ik}(y)\cos(k\chi)\sigma^i + o(\sigma^{q-1})\right). \tag{32}$$

3 SOLUTION UP TO THE FIRST ORDER

To this order, we shall show the calculation in detail. The unknown quantities are β_{11}, Ω_0, Ω_1, Ω_2 and v_0. The surface function reads

$$r_{\mathrm{s}}(\chi) = a[1 + \beta_{11}\sigma\cos\chi + o(\sigma)] \tag{33}$$

and equation (12) becomes

$$\int\limits_0^{2\pi} r_{\mathrm{s}}(\chi)^3 \cos\chi\,\mathrm{d}\chi = a^3[3\pi\beta_{11}\sigma + o(\sigma)]. \tag{34}$$

This gives

$$\beta_{11} = 0, \tag{35}$$

cf. Table A2, which means that we have the surface function

$$r_{\mathrm{s}}(\chi) = a[1 + o(\sigma)]. \tag{36}$$

Next we have to evaluate equation (10). We immediately see that

$$\Omega_0 = \Omega_1 = 0 \tag{37}$$

must hold, and furthermore we have

$$\frac{1}{2}\Omega^2\varrho^2\Big|_{\mathrm{s}} = \pi G\mu a^2\left[\frac{\Omega_2}{2} + \left(\frac{\Omega_3}{2} - \Omega_2\cos\chi\right)\sigma + o(\sigma)\right] \tag{38}$$

at the surface. To calculate the potential at the ring's surface to the same order in σ, we first compute the potential along the axis. Here we have to calculate the potential of a torus[2]:

$$\begin{aligned} U_{\mathrm{axis}}(R) = -\frac{8\pi G\mu a^3}{3R}\Bigg[&\left(1 + \frac{R^2}{a^2}\right)E\left(\frac{a}{R}\right)\sigma^{-1} \\ &+ \left(1 - \frac{R^2}{a^2}\right)K\left(\frac{a}{R}\right)\sigma^{-1} + o(1)\Bigg]. \end{aligned} \tag{39}$$

The expansion in terms of powers of $1/R$ gives

$$A_1 = 1 + o(\sigma), \tag{40}$$

---

[2] E denotes the complete elliptic integral of the second kind, $E(k) := \int_0^{\frac{\pi}{2}} \sqrt{1 - k^2\sin^2\theta}\,\mathrm{d}\theta$.

and

$$A_2 = -\frac{1}{8}\sigma + o(\sigma), \tag{41}$$

thus

$$\alpha_{10} = 1, \quad \alpha_{11} = 0 \quad \text{and} \quad \alpha_{21} = -\frac{1}{8}, \tag{42}$$

cf. Table A4. Now we are able to calculate the potential at the body's surface via (27), (28) and the corresponding equation for I_2. Using equation (36) it is possible to expand the surface potential in σ. We get

$$U_\mathrm{s}(\chi) = -2\pi G\mu a^2 \left[\lambda + 2 + \left(\frac{\lambda}{2} + \frac{3}{8}\right)\sigma\cos\chi + o(\sigma)\right], \tag{43}$$

which implies

$$\phi_{00} = \lambda + 2, \quad \phi_{10} = 0 \quad \text{and} \quad \phi_{11} = \frac{\lambda}{2} + \frac{3}{8}. \tag{44}$$

Plugging (16), (38) and (43) into equation (10) and collecting the coefficients in $\sigma^i\cos(k\chi)$, we find the following equations:

i	k	equation
0	0	$2\lambda + 4 + \frac{1}{2}\Omega_2 = v_0$
1	0	$\frac{1}{2}\Omega_3 = v_1$
1	1	$\lambda + \frac{3}{4} - \Omega_2 = 0$

Solving these equations gives

$$\Omega_2 = \lambda + \tfrac{3}{4}, \tag{45}$$

cf. Table A1, and

$$v_0 = \tfrac{5}{2}\lambda + \tfrac{35}{8}. \tag{46}$$

The equation with Ω_3 and v_1 cannot be further evaluated until the next order $q = 2$.

For the mass and the angular momentum, we get

$$M = 2\pi^2\mu a^3[\sigma^{-1} + o(\sigma^{-1})] \tag{47}$$

and

$$J = \sqrt{\pi^5 G\mu^3(4\lambda + 3)}\, a^5[\sigma^{-2} + o(\sigma^{-2})]. \tag{48}$$

To leading order, $\varrho_\mathrm{i}/\varrho_\mathrm{o} = 1 - 2\sigma$ holds, and we can conclude that

$$\lim_{\varrho_\mathrm{i}/\varrho_\mathrm{o}\to 1}\left[\frac{4\pi b V_0}{5GM} - \ln\left(1 - \frac{\varrho_\mathrm{i}}{\varrho_\mathrm{o}}\right)\right] = \frac{1}{4} - \ln 16, \tag{49}$$

see also equation (11) in Fischer, Horatschek & Ansorg (2005). A comparison of this result for homogeneous rings with the analogue for polytropic rings can be found in Petroff & Horatschek (2008).

To calculate the inner potential, we have to find a solution to Poisson's equation. The ansatz (31) leads to the ODE

$$\frac{\mathrm{d}^2U_{00}(y)}{\mathrm{d}y^2} + \frac{1}{y}\frac{\mathrm{d}U_{00}(y)}{\mathrm{d}y} + 4 = 0 \tag{50}$$

to leading order, which has the solution

$$U_{00}(y) = -y^2 + C_1\ln y + C_2. \tag{51}$$

At the centre, the potential has to be regular, thus $C_1 = 0$. The resulting potential at the surface $r = r_\mathrm{s}(\chi)$ is

$$U_\mathrm{s}(\chi) = \pi G\mu a^2[1 - C_2 + o(1)]. \tag{52}$$

For the potential to be continuous, $C_2 = 2\lambda + 5$ must hold, see (43). To the zeroth order the potential is not a function of the angle χ.

Furthermore we have the equations

$$\frac{\mathrm{d}^2U_{10}(y)}{\mathrm{d}y^2} + \frac{1}{y}\frac{\mathrm{d}U_{10}(y)}{\mathrm{d}y} = 0 \tag{53}$$

and

$$\frac{\mathrm{d}^2U_{11}(y)}{\mathrm{d}y^2} + \frac{1}{y}\frac{\mathrm{d}U_{11}(y)}{\mathrm{d}y} - \frac{U_{11}(y)}{y^2} + 2y = 0. \tag{54}$$

Note that the $2y$ term in the second equation results from $U_{00}(y)$, which is already known. The solutions of these equations that are regular at the centre and have the correct values at the surface are

$$U_{10}(y) = 0 \tag{55}$$

and

$$U_{11}(y) = (\lambda + 1)y - \frac{y^3}{4}, \tag{56}$$

cf. Table A3. For the pressure, (9) leads to

$$p_{00}(y) = 1 - y^2, \tag{57}$$

$$p_{10}(y) = 0 \tag{58}$$

and

$$p_{11}(y) = \frac{y}{4} - \frac{y^3}{4}. \tag{59}$$

After finding the inner potential and pressure, we can calculate the potential energy

$$W := \frac{\mu}{2}\int U\,\mathrm{d}V = -\pi^3 G\mu^2 a^5\left[\left(2\lambda + \frac{9}{2}\right)\sigma^{-1} + o(\sigma^{-1})\right],$$

the rotational energy

$$T := \frac{\mu\Omega^2}{2}\int \varrho^2\,\mathrm{d}V = \pi^3 G\mu^2 a^5\left[\left(\lambda + \frac{3}{4}\right)\sigma^{-1} + o(\sigma^{-1})\right]$$

and the integral over the pressure

$$P := \int p\,\mathrm{d}V = \pi^3 G\mu^2 a^5\left(\sigma^{-1} + o(\sigma^{-1})\right) \tag{60}$$

to first order. We see that the virial theorem (62) is fulfilled up to this order.

4 DISCUSSION

With this approximation method, we are able to calculate e.g. the shape, angular velocity and pressure of the ring up to arbitrary order in σ. We have done so up to the 20th order.

To test our solutions, we ensured that the transition condition

$$\nabla U_\mathrm{in}|_\mathrm{s} = \nabla U_\mathrm{out}|_\mathrm{s} \tag{61}$$

Table 1. For a given radius ratio $\varrho_\mathrm{i}/\varrho_\mathrm{o} = 0.9$, physical quantities to different orders in q and numerically determined values are compared to the values for $q = 20$: $\bar{M}_{20} = 4.6299179884304816293 \times 10^{-2}$, $\bar{\Omega}^2_{20} = 3.2474683264953211610 \times 10^{-2}$, $\bar{J}_{20} = 7.5456215256289320669 \times 10^{-3}$, $\bar{P}_{20} = 1.7862946528142761708 \times 10^{-4}$, $\bar{T}_{20} = 6.7988816964653749490 \times 10^{-4}$, $\bar{W}_{20} = -1.8956647351373578410 \times 10^{-3}$.

q	σ	$\bar{M}_q/\bar{M}_{20} - 1$	$\bar{\Omega}^2_q/\bar{\Omega}^2_{20} - 1$	$\bar{J}_q/\bar{J}_{20} - 1$	$\bar{P}_q/\bar{P}_{20} - 1$	$\bar{T}_q/\bar{T}_{20} - 1$	$\bar{W}_q/\bar{W}_{20} - 1$
1	0.053	1×10^{-2}	1×10^{-2}	2×10^{-2}	3×10^{-2}	2×10^{-2}	2×10^{-2}
2	0.052	2×10^{-4}	6×10^{-4}	4×10^{-4}	6×10^{-3}	-1×10^{-3}	6×10^{-4}
3	0.052	2×10^{-4}	1×10^{-4}	2×10^{-4}	4×10^{-4}	3×10^{-4}	3×10^{-4}
4	0.052	3×10^{-6}	-1×10^{-5}	-3×10^{-6}	5×10^{-5}	-5×10^{-5}	-2×10^{-5}
10	0.052	6×10^{-11}	-9×10^{-11}	4×10^{-12}	5×10^{-10}	-6×10^{-10}	-3×10^{-10}
19	0.052	4×10^{-17}	4×10^{-17}	6×10^{-17}	1×10^{-16}	9×10^{-17}	9×10^{-17}
num	—	-4×10^{-14}	1×10^{-16}	-4×10^{-14}	-7×10^{-14}	-4×10^{-14}	-3×10^{-14}

Table 2. For a given radius ratio $\varrho_\mathrm{i}/\varrho_\mathrm{o} = 0.5$, physical quantities to different orders in q are compared to the numerically determined values $\bar{M}_\mathrm{num} = 0.7201292$, $\bar{\Omega}^2_\mathrm{num} = 0.5467604$, $\bar{J}_\mathrm{num} = 0.3247949$, $\bar{P}_\mathrm{num} = 0.04874713$, $\bar{T}_\mathrm{num} = 0.1200820$, $\bar{W}_\mathrm{num} = -0.3864053$.

q	σ	$\bar{M}_q/\bar{M}_\mathrm{num} - 1$	$\bar{\Omega}^2_q/\bar{\Omega}^2_\mathrm{num} - 1$	$\bar{J}_q/\bar{J}_\mathrm{num} - 1$	$\bar{P}_q/\bar{P}_\mathrm{num} - 1$	$\bar{T}_q/\bar{T}_\mathrm{num} - 1$	$\bar{W}_q/\bar{W}_\mathrm{num} - 1$
1	0.33	2.8×10^{-1}	2.3×10^{-1}	4.2×10^{-1}	8.6×10^{-1}	4.6×10^{-1}	6.1×10^{-1}
2	0.30	5.1×10^{-2}	5.9×10^{-2}	6.5×10^{-2}	2.5×10^{-1}	2.6×10^{-2}	1.1×10^{-1}
3	0.30	5.1×10^{-2}	4.2×10^{-2}	5.8×10^{-2}	1.3×10^{-1}	8.1×10^{-2}	1.0×10^{-1}
4	0.30	1.7×10^{-2}	1.3×10^{-2}	1.9×10^{-2}	5.4×10^{-2}	8.4×10^{-3}	2.6×10^{-2}
10	0.29	1.2×10^{-3}	1.0×10^{-3}	1.3×10^{-3}	3.2×10^{-3}	1.0×10^{-3}	1.9×10^{-3}
20	0.29	2.6×10^{-5}	2.5×10^{-5}	3.0×10^{-5}	7.2×10^{-5}	2.7×10^{-5}	4.4×10^{-5}

is fulfilled up to the appropriate order in σ. Furthermore we tested that the virial theorem

$$W + 2T + 3P = 0 \tag{62}$$

is fulfilled for each order in σ.

An important question is how good this method is. In Tables 1, 2 and 3 one can see how the dimensionless quantities

$$\begin{gathered}\frac{\bar{M}}{M} = \frac{1}{\mu\varrho_\mathrm{o}^3}, \qquad \frac{\bar{\Omega}^2}{\Omega^2} = \frac{1}{G\mu}, \qquad \frac{\bar{J}}{J} = \frac{1}{G^{1/2}\mu^{3/2}\varrho_\mathrm{o}^5}, \\ \frac{\bar{P}}{P} = \frac{\bar{T}}{T} = \frac{\bar{W}}{W} = \frac{1}{G\mu^2\varrho_\mathrm{o}^5}\end{gathered} \tag{63}$$

improve in accuracy with increasing order for different radius ratios. Especially for thin rings, we get very accurate results. In fact, for rings with radius ratios $\varrho_\mathrm{i}/\varrho_\mathrm{o} \approx 0.85$ we achieve a precision which is comparable with that given by the numerical method described in Ansorg, Kleinwächter & Meinel (2003a). For larger radius ratios, the accuracy is thus better. As a co-product, our work provides an independent test of the accuracy of the numerical method (better than 10^{-13} cf. Table 1).

The shape of the ring in meridional cross-section for various radius ratios can be found in Fig. 2. The curves to order $q = 20$ can barely be distinguished from the numerical ones for $\varrho_\mathrm{i}/\varrho_\mathrm{o} \gtrsim 0.3$. As one approaches the transition to spheroidal topologies ($\varrho_\mathrm{i}/\varrho_\mathrm{o} \to 0$), the true curve becomes pointy at the inner edge and is no longer well represented by our Fourier series. Nevertheless, the shape of the ring is quite well approximated even for $\varrho_\mathrm{i}/\varrho_\mathrm{o} = 0.1$, as seen in Fig. 3. The surface function $r_\mathrm{s}(\chi)$, which is a constant to leading order, clearly approaches the numerical one with increasing q. The pressure in the equatorial plane can also be seen to approach the numerically determined one for $\varrho_\mathrm{i}/\varrho_\mathrm{o} = 0.3$ in Fig. 4. It is interesting to note that the centre of mass does not coincide with the point of maximum pressure.

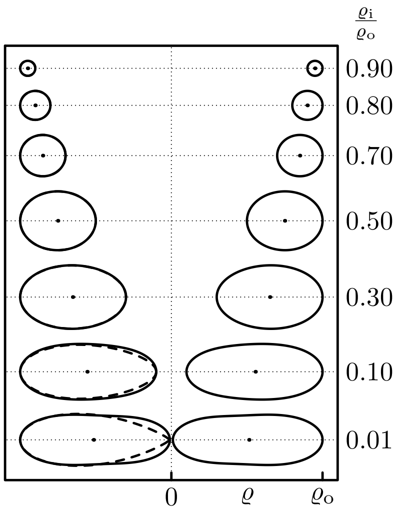

Figure 2. Meridional cross-sections of rings to the order $q = 20$ for different radius ratios $\varrho_\mathrm{i}/\varrho_\mathrm{o}$. The ϱ- and z-axis are scaled identically in such a manner that ϱ_o has the same value for all the rings. The dot in each ring marks the centre of mass of the cross-section ($\varrho = b, z = 0$ i.e. $r = 0$) and the dashed line shows the numerical result and is indistinguishable from the $q = 20$ curve for $\varrho_\mathrm{i}/\varrho_\mathrm{o} \gtrsim 0.3$.

In Fig. 5 one can get an impression of the accuracy of the approximation over the whole range of radius ratios and for various values of q. Despite the claim found in Wong (1974) that Dyson's perturbative method diverges for $\sigma > 1/3$ (see also the comments in Dyson 1892), these results indicate the opposite.

The (dimensionless) coefficients β_{ik} and Ω_i are only functions of the dimensionless quantity $\sigma = a/b$, but not of any length like ϱ_o for example. The reason for this is that

Table 3. For a given radius ratio $\varrho_\mathrm{i}/\varrho_\mathrm{o} = 0.2$, physical quantities to different orders in q are compared to the numerically determined values $\bar{M}_\mathrm{num} = 0.9424$, $\bar{\Omega}^2_\mathrm{num} = 0.9844$, $\bar{J}_\mathrm{num} = 0.4545$, $\bar{P}_\mathrm{num} = 0.07865$, $\bar{T}_\mathrm{num} = 0.2255$, $\bar{W}_\mathrm{num} = -0.6869$.

q	σ	$\bar{M}_q/\bar{M}_\mathrm{num} - 1$	$\bar{\Omega}^2_q/\bar{\Omega}^2_\mathrm{num} - 1$	$\bar{J}_q/\bar{J}_\mathrm{num} - 1$	$\bar{P}_q/\bar{P}_\mathrm{num} - 1$	$\bar{T}_q/\bar{T}_\mathrm{num} - 1$	$\bar{W}_q/\bar{W}_\mathrm{num} - 1$
1	0.67	1.0	7.5×10^{-1}	1.6	5.1	1.6	2.8
2	0.54	3.2×10^{-1}	3.5×10^{-1}	3.9×10^{-1}	1.6	3.2×10^{-1}	7.6×10^{-1}
3	0.54	3.2×10^{-1}	2.7×10^{-1}	3.5×10^{-1}	1.1	5.4×10^{-1}	7.2×10^{-1}
4	0.51	1.9×10^{-1}	1.7×10^{-1}	2.1×10^{-1}	6.3×10^{-1}	2.1×10^{-1}	3.6×10^{-1}
10	0.47	6.4×10^{-2}	6.9×10^{-2}	7.1×10^{-2}	1.9×10^{-1}	8.7×10^{-2}	1.2×10^{-1}
20	0.46	2.2×10^{-2}	2.7×10^{-2}	2.3×10^{-2}	6.0×10^{-2}	3.2×10^{-2}	4.2×10^{-2}

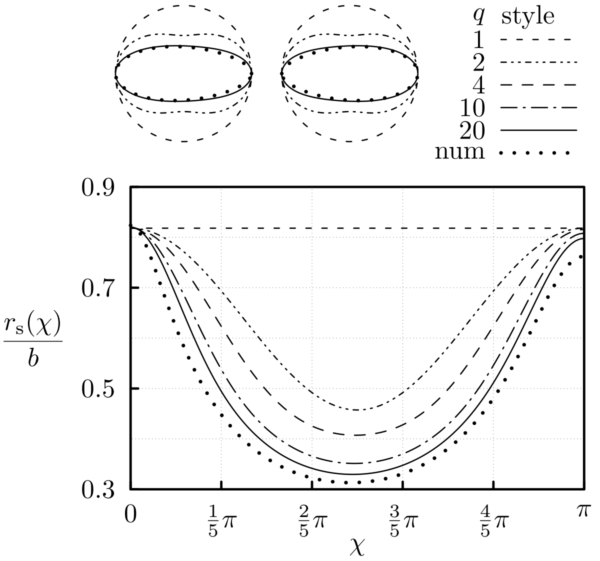

Figure 3. The meridional cross-section and the (dimensionless) surface function $r_\mathrm{s}(\chi)/b$ of the ring with radius ratio $\varrho_\mathrm{i}/\varrho_\mathrm{o} = 0.1$ for different orders q compared to the numerical result. The surfaces are scaled such that ϱ_o (and therefore also ϱ_i) has the same value to all orders.

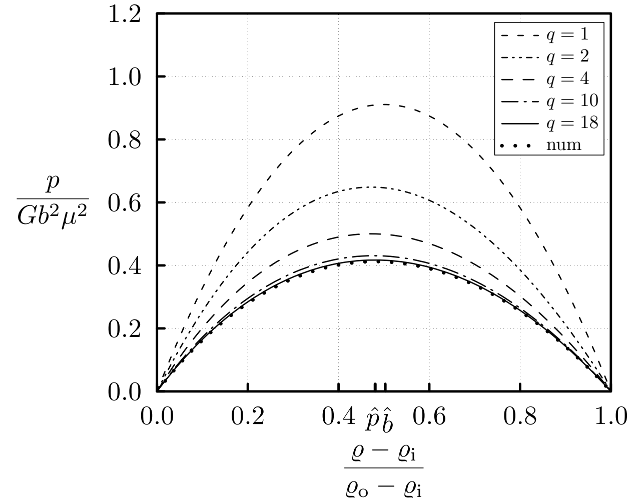

Figure 4. The pressure in the equatorial plane for a ring with radius ratio $\varrho_\mathrm{i}/\varrho_\mathrm{o} = 0.3$ for different orders q compared to the numerical result. It is interesting to note that the centre of mass of the cross-section does not coincide with the point of maximum pressure. To the order $q = 18$ we get $\hat{b} := (b - \varrho_\mathrm{i})/(\varrho_\mathrm{o} - \varrho_\mathrm{i}) = 0.503$ and $\hat{p} := (\varrho_{\mathrm{p,max}} - \varrho_\mathrm{i})/(\varrho_\mathrm{o} - \varrho_\mathrm{i}) = 0.480$, which differ by less than 1% from the numerical values.

equations (4), (5), (6) and (11) are scale invariant in the following sense: If $U(\boldsymbol{x})$, $\mu(\boldsymbol{x})$, $p(\boldsymbol{x})$ and $\boldsymbol{v}(\boldsymbol{x})$ are solutions of these equations then $\alpha^{-2}U(\alpha\boldsymbol{x})$, $\mu(\alpha\boldsymbol{x})$, $\alpha^{-2}p(\alpha\boldsymbol{x})$ and $\alpha^{-1}\boldsymbol{v}(\alpha\boldsymbol{x})$ are too, where α is an arbitrary scaling factor. Other equations of state $\mu = \mu(p)$ will not satisfy this scaling invariance in general. To parametrize a specific ring, including its dimension, we need two parameters (for example σ and b) as expected.

Please note that one has to be careful in interpreting the results for the thin ring limit. For example, one might think that the squared angular velocity vanishes like $\sigma^2 \ln \sigma$. This is true for the dimensionless quantity $\Omega^2/G\mu$, but need not be true for the squared angular velocity itself. If we fix the 'size' b and the mass M of the ring in that limit, then the cross-section shrinks to a point ($a = \sigma b$). With (47) we can conclude that $\mu \propto \sigma^{-2}$ and therefore $\Omega^2 \propto \ln \sigma$, which means that Ω^2 and hence the velocity of a fluid element go to infinity.

Relativistic rings, including the thin ring limit, were studied in Ansorg, Kleinwächter & Meinel (2003b), Ansorg et al. (2004) and Fischer et al. (2005). From the perspective of General Relativity, the Newtonian theory constitutes a good approximation when certain conditions are fulfilled. For one thing, typical velocities must be small compared to the speed of light and for another $G|U| \ll c^2$ must hold. We just saw, however, that for rings of finite extent and mass, the velocities grow unboundedly in the thin ring limit. The same holds for U_s as well, see (52). This means that the Newtonian theory of gravity is not appropriate to describe this subtle limit itself, since one cannot expect it to be a good approximation to General Relativity. It is remarkable that the approximation about the point $\sigma = 0$ is nevertheless so successful.

ACKNOWLEDGMENTS

It is a pleasure to thank Reinhard Meinel for fruitful discussions. This research was funded in part by the Deutsche Forschungsgemeinschaft (SFB/TR7–B1).

REFERENCES

Ansorg M., Fischer T., Kleinwächter A., Meinel R., Petroff D., Schöbel K., 2004, Mon. Not. R. Astron. Soc., 355, 682

Ansorg M., Kleinwächter A., Meinel R., 2003a, Astron. Astrophys., 405, 711

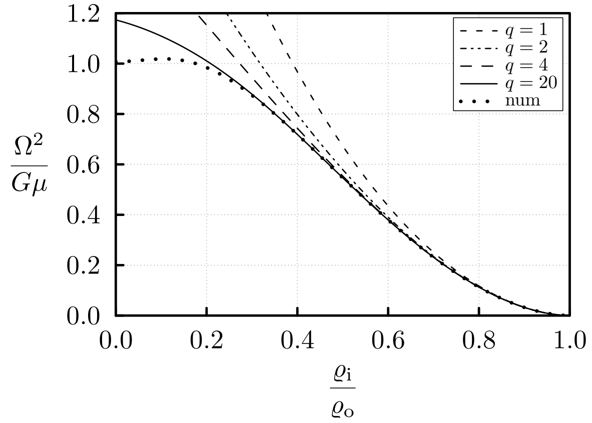

Figure 5. The (dimensionless) squared angular velocity $\Omega^2/G\mu$ as function of the radius ratio $\varrho_\mathrm{i}/\varrho_\mathrm{o}$ for different orders q compared to the numerical result.

Ansorg M., Kleinwächter A., Meinel R., 2003b, Astrophys. J. Lett., 582, L87
Ansorg M., Kleinwächter A., Meinel R., 2003c, Mon. Not. R. Astron. Soc., 339, 515
Ansorg M., Petroff D., 2005, Phys. Rev. D, 72, 024019
Dyson F. W., 1892, Philos. Trans. R. Soc. London, Ser. A, 184, 43
Dyson F. W., 1893, Philos. Trans. R. Soc. London, Ser. A, 184, 1041
Eriguchi Y., Hachisu I., 1985, Astron. Astrophys., 148, 289
Eriguchi Y., Sugimoto D., 1981, Prog. Theor. Phys., 65, 1870
Fischer T., Horatschek S., Ansorg M., 2005, Mon. Not. R. Astron. Soc., 364, 943
Kowalewsky S., 1885, Astronomische Nachrichten, 111, 37
Lichtenstein L., 1933, Gleichgewichtsfiguren rotierender Flüssigkeiten. Springer, Berlin
Petroff D., Horatschek S., 2008, `arXiv:0802.0081`
Poincaré H., 1885, Acta mathematica, 7, 259
Wong C. Y., 1974, Astrophys. J., 190, 675

APPENDIX A: FURTHER COEFFICIENTS

In Tables A1–A4, coefficients for Ω_i, β_{ik}, $U_{ik}(y)$ and α_{li} are given.

Table A1. Coefficients Ω_i up to the order $q = 9$ ($i = 2, 3, \ldots, 10$).

i	Ω_i
2	$\lambda + \frac{3}{4}$
3	0
4	$-\frac{1}{8}\,\lambda - \frac{19}{96}$
5	0
6	$\frac{25}{128}\,\lambda^3 + \frac{365}{1536}\,\lambda^2 - \frac{2345}{18432}\,\lambda - \frac{8989}{73728}$
7	0
8	$\frac{25}{64}\,\lambda^4 + \frac{40235}{98304}\,\lambda^3 - \frac{134255}{294912}\,\lambda^2 - \frac{36493505}{56623104}\,\lambda - \frac{34831813}{226492416}$
9	0
10	$\frac{134925}{131072}\,\lambda^5 + \frac{2797535}{1572864}\,\lambda^4 - \frac{50072105}{169869312}\,\lambda^3 -$ $\frac{1021727845}{509607936}\,\lambda^2 - \frac{104581877693}{97844723712}\,\lambda - \frac{49377918425}{391378894848}$

Table A2. Coefficients β_{ik} up to the order $q = 9$. The bold-faced type indicates that these terms are incorrect in Dyson (1892).

$i \backslash k$	1	2	3	4	5	6	7	8	9
1	0	—	—	—	—	—	—	—	—
2	0	$\frac{5}{8}\lambda + \frac{35}{96}$	—	—	—	—	—	—	—
3	0	0	$\frac{5}{128}\lambda - \frac{35}{3072}$	—	—	—	—	—	—
4	0	$\frac{5}{8}\lambda^2 +$ $\mathbf{\frac{95}{128}}\lambda + \mathbf{\frac{1145}{9216}}$	0	$\frac{75}{256}\lambda^2 +$ $\mathbf{\frac{815}{2304}}\lambda + \mathbf{\frac{5089}{55296}}$	—	—	—	—	—
5	$-\frac{25}{1024}\lambda^2 -$ $\frac{175}{24576}\lambda +$ $\frac{1225}{294912}$	0	$\frac{15}{256}\lambda^2 +$ $\frac{4955}{147456}\lambda -$ $\frac{62141}{3538944}$	0	$\frac{25}{512}\lambda^2 +$ $\frac{75}{4096}\lambda -$ $\frac{14455}{1179648}$	—	—	—	—
6	0	$\frac{5185}{4096}\lambda^3 +$ $\frac{110515}{49152}\lambda^2 +$ $\frac{853225}{884736}\lambda +$ $\frac{34487}{1327104}$	0	$\frac{75}{128}\lambda^3 +$ $\frac{116545}{110592}\lambda^2 +$ $\frac{308395}{589824}\lambda +$ $\frac{17892169}{318504960}$	0	$\frac{625}{4096}\lambda^3 +$ $\frac{169625}{589824}\lambda^2 +$ $\frac{1097461}{7077888}\lambda +$ $\frac{7327349}{339738624}$	—	—	—
7	$-\frac{125}{2048}\lambda^3 -$ $\frac{76325}{1179648}\lambda^2 +$ $\frac{78175}{28311552}\lambda +$ $\frac{1313095}{169869312}$	0	$\frac{1325}{8192}\lambda^3 +$ $\frac{109915}{442368}\lambda^2 +$ $\frac{863633}{18874368}\lambda -$ $\frac{105833029}{4076863488}$	0	$\frac{125}{1024}\lambda^3 +$ $\frac{9815}{73728}\lambda^2 -$ $\frac{472843}{56623104}\lambda -$ $\frac{32985941}{1509949440}$	0	$\frac{375}{8192}\lambda^3 +$ $\frac{4825}{98304}\lambda^2 -$ $\frac{34745}{9437184}\lambda -$ $\frac{268795}{28311552}$	—	—
8	0	$\frac{11935}{4096}\lambda^4 +$ $\frac{15693265}{2359296}\lambda^3 +$ $\frac{387327415}{84934656}\lambda^2 +$ $\frac{1967050099}{2717908992}\lambda -$ $\frac{21240691225}{195689447424}$	0	$\frac{48175}{32768}\lambda^4 +$ $\frac{299613275}{84934656}\lambda^3 +$ $\frac{86354441}{31850496}\lambda^2 +$ $\frac{163195481003}{244611809280}\lambda +$ $\frac{61946667647}{14676708556800}$	0	$\frac{1875}{4096}\lambda^4 +$ $\frac{1994875}{1769472}\lambda^3 +$ $\frac{1544984219}{1698693120}\lambda^2 +$ $\frac{26196760631}{101921587200}\lambda +$ $\frac{523810097561}{34245653299200}$	0	$\frac{21875}{262144}\lambda^4 +$ $\frac{2069375}{9437184}\lambda^3 +$ $\frac{7862435}{42467328}\lambda^2 +$ $\frac{6142108445}{114152177664}\lambda +$ $\frac{968695327}{342456532992}$	—
9	$-\frac{26875}{131072}\lambda^4 -$ $\frac{10803575}{28311552}\lambda^3 -$ $\frac{73205885}{452984832}\lambda^2 +$ $\frac{245384393}{10871635968}\lambda +$ $\frac{5148689159}{391378894848}$	0	$\frac{58565}{131072}\lambda^4 +$ $\frac{317810795}{339738624}\lambda^3 +$ $\frac{4061560685}{8153726976}\lambda^2 -$ $\frac{3261000013}{97844723712}\lambda -$ $\frac{1033257753043}{23482733690880}$	0	$\frac{3125}{8192}\lambda^4 +$ $\frac{20750915}{28311552}\lambda^3 +$ $\frac{738672683}{2264924160}\lambda^2 -$ $\frac{180456831247}{3261490790400}\lambda -$ $\frac{13297677452861}{365286968524800}$	0	$\frac{2625}{16384}\lambda^4 +$ $\frac{2597725}{9437184}\lambda^3 +$ $\frac{112005563}{1358954496}\lambda^2 -$ $\frac{117378627479}{2283043553280}\lambda -$ $\frac{173703027451}{9132174213120}$	0	$\frac{625}{16384}\lambda^4 +$ $\frac{72125}{1048576}\lambda^3 +$ $\frac{4955105}{226492416}\lambda^2 -$ $\frac{79046365}{5435817984}\lambda -$ $\frac{1636799939}{260919263232}$

Table A3. Coefficients $U_{ik}(y)$ up to the order $q = 7$.

$i \backslash k$	0	1	2	3	4	5	6	7
0	$2\lambda+5-y^2$	—	—	—	—	—	—	—
1	0	$(\lambda+1)y-\frac{1}{4}y^3$	—	—	—	—	—	—
2	$-\frac{1}{8}\lambda-\frac{7}{32}+(\frac{1}{4}\lambda+\frac{1}{4})y^2-\frac{3}{32}y^4$	0	$(\lambda+\frac{31}{48})y^2-\frac{5}{48}y^4$	—	—	—	—	—
3	0	$(-\frac{13}{32}\lambda-\frac{65}{192})y+(\frac{7}{16}\lambda+\frac{67}{192})y^3-\frac{15}{128}y^5$	0	$(\frac{15}{64}\lambda+\frac{175}{1536})y^3-\frac{35}{768}y^5$	—	—	—	—
4	$\frac{25}{64}\lambda^3+\frac{295}{384}\lambda^2+\frac{3457}{9216}\lambda+\frac{19}{576}+(-\frac{13}{128}\lambda-\frac{65}{768})y^2+(\frac{21}{128}\lambda+\frac{67}{512})y^4-\frac{25}{512}y^6$	0	$(\frac{5}{8}\lambda^2+\frac{311}{512}\lambda+\frac{269}{36864})y^2+(\frac{185}{768}\lambda+\frac{3205}{18432})y^4-\frac{35}{512}y^6$	0	$(\frac{455}{4608}\lambda+\frac{4459}{110592})y^4-\frac{21}{1024}y^6$	—	—	—
5	0	$(\frac{25}{128}\lambda^3-\frac{355}{1536}\lambda^2-\frac{20005}{36864}\lambda-\frac{11081}{73728})y+(\frac{5}{32}\lambda^2+\frac{155}{2048}\lambda-\frac{9091}{147456})y^3+(\frac{465}{2048}\lambda+\frac{2855}{16384})y^5-\frac{875}{12288}y^7$	0	$(\frac{15}{256}\lambda^2+\frac{25}{73728}\lambda-\frac{100015}{1769472})y^3+(\frac{4795}{36864}\lambda+\frac{76223}{884736})y^5-\frac{315}{8192}y^7$	0	$(\frac{805}{18432}\lambda+\frac{26579}{1769472})y^5-\frac{77}{8192}y^7$	—	—
6	$\frac{25}{32}\lambda^4+\frac{95435}{49152}\lambda^3+\frac{862135}{589824}\lambda^2+\frac{7959115}{28311552}\lambda-\frac{551045}{28311552}+(\frac{25}{512}\lambda^3-\frac{355}{6144}\lambda^2-\frac{20005}{147456}\lambda-\frac{11081}{294912})y^2+(\frac{15}{256}\lambda^2+\frac{465}{16384}\lambda-\frac{9091}{393216})y^4+(\frac{775}{8192}\lambda+\frac{14275}{196608})y^6-\frac{6125}{196608}y^8$	0	$(\frac{335}{256}\lambda^3+\frac{9895}{4608}\lambda^2+\frac{440125}{589824}\lambda-\frac{1755973}{42467328})y^2+(\frac{245}{3072}\lambda^2+\frac{9325}{294912}\lambda-\frac{31315}{786432})y^4+(\frac{455}{3072}\lambda+\frac{32011}{294912})y^6-\frac{1575}{32768}y^8$	0	$(\frac{125}{6912}\lambda^2-\frac{2765}{1769472}\lambda-\frac{1824697}{79626240})y^4+(\frac{10241}{147456}\lambda+\frac{1504909}{35389440})y^6-\frac{693}{32768}y^8$	0	$(\frac{17549}{884736}\lambda+\frac{243479}{42467328})y^6-\frac{143}{32768}y^8$	—
7	0	$(\frac{25}{64}\lambda^4-\frac{40645}{98304}\lambda^3-\frac{2042065}{1179648}\lambda^2-\frac{58120985}{56623104}\lambda-\frac{39130979}{339738624})y+(\frac{745}{2048}\lambda^3+\frac{36385}{73728}\lambda^2+\frac{200065}{2359296}\lambda-\frac{6542965}{169869312})y^3+(\frac{645}{8192}\lambda^2+\frac{27925}{786432}\lambda-\frac{645475}{18874368})y^5+(\frac{85225}{589824}\lambda+\frac{1539545}{14155776})y^7-\frac{25725}{524288}y^9$	0	$(\frac{1485}{8192}\lambda^3+\frac{439675}{1769472}\lambda^2-\frac{246977}{28311552}\lambda-\frac{513938083}{10192158720})y^3+(\frac{17435}{442368}\lambda^2+\frac{190295}{14155776}\lambda-\frac{117973177}{5096079360})y^5+(\frac{36449}{393216}\lambda+\frac{6114493}{94371840})y^7-\frac{8085}{262144}y^9$	0	$(\frac{12385}{1769472}\lambda^2+\frac{35497}{28311552}\lambda-\frac{181782779}{20384317440})y^5+(\frac{5425}{147456}\lambda+\frac{2961899}{141557760})y^7-\frac{3003}{262144}y^9$	0	$(\frac{32417}{3538944}\lambda+\frac{375383}{169869312})y^7-\frac{2145}{1048576}y^9$

Table A4. Coefficients α_{li} up to the order $q = 8$.

$l \backslash i$	0	1	2	3	4	5	6	7	8
1	1	0	0	0	$\frac{25}{128}\lambda^2 + \frac{175}{768}\lambda + \frac{1225}{18432}$	0	$\frac{25}{64}\lambda^3 + \frac{68075}{98304}\lambda^2 + \frac{410275}{1179648}\lambda + \frac{2568475}{56623104}$	0	$\frac{134925}{131072}\lambda^4 + \frac{239525}{98304}\lambda^3 + \frac{316929175}{169869312}\lambda^2 + \frac{1001961695}{2038431744}\lambda + \frac{2116102111}{97844723712}$
2	—	$-\frac{1}{8}$	0	$-\frac{25}{32}\lambda - \frac{175}{384}$	0	$-\frac{475}{512}\lambda^2 - \frac{555}{512}\lambda - \frac{965}{4608}$	0	$-\frac{10025}{4096}\lambda^3 - \frac{1698785}{393216}\lambda^2 - \frac{28823195}{14155776}\lambda - \frac{123632507}{679477248}$	0
3	—	—	$\frac{5}{16}\lambda + \frac{17}{96}$	0	$\frac{5}{16}\lambda^2 + \frac{1315}{3072}\lambda + \frac{9235}{73728}$	0	$\frac{1765}{2048}\lambda^3 + \frac{1985}{1024}\lambda^2 + \frac{4356505}{3538944}\lambda + \frac{18119345}{84934656}$	0	$\frac{2195}{1024}\lambda^4 + \frac{3052455}{524288}\lambda^3 + \frac{888829145}{169869312}\lambda^2 + \frac{515947105}{301989888}\lambda + \frac{13524934807}{97844723712}$
4	—	—	—	$-\frac{5}{256}\lambda - \frac{107}{6144}$	0	$-\frac{475}{1536}\lambda^2 - \frac{323095}{884736}\lambda - \frac{2199527}{21233664}$	0	$-\frac{15815}{24576}\lambda^3 - \frac{6138925}{5308416}\lambda^2 - \frac{71128549}{113246208}\lambda - \frac{12275264429}{122305904640}$	0
5	—	—	—	—	$\frac{25}{768}\lambda^2 + \frac{515}{13824}\lambda + \frac{13777}{1327104}$	0	$\frac{25}{384}\lambda^3 + \frac{163145}{1327104}\lambda^2 + \frac{62041}{786432}\lambda + \frac{133449991}{7644119040}$	0	$\frac{20225}{98304}\lambda^4 + \frac{81963095}{127401984}\lambda^3 + \frac{260962627}{382205952}\lambda^2 + \frac{10908318845}{36691771392}\lambda + \frac{1946363428441}{44030125670400}$
6	—	—	—	—	—	$-\frac{25}{24576}\lambda^2 - \frac{3749}{1769472}\lambda - \frac{384013}{424673280}$	0	$-\frac{425}{12288}\lambda^3 - \frac{5290135}{84934656}\lambda^2 - \frac{82443283}{2264924160}\lambda - \frac{6684148507}{978447237120}$	0
7	—	—	—	—	—	—	$\frac{125}{73728}\lambda^3 + \frac{20765}{7077888}\lambda^2 + \frac{77707}{47185920}\lambda + \frac{6177187}{20384317440}$	0	$\frac{125}{24576}\lambda^4 + \frac{515945}{42467328}\lambda^3 + \frac{1166591837}{101921587200}\lambda^2 + \frac{62067170651}{12230590464000}\lambda + \frac{3643667826661}{4109478395904000}$
8	—	—	—	—	—	—	—	$-\frac{25}{1179648}\lambda^3 - \frac{595}{6291456}\lambda^2 - \frac{619081}{6794772480}\lambda - \frac{28211731}{1141521776640}$	0
9	—	—	—	—	—	—	—	—	$\frac{125}{2359296}\lambda^4 + \frac{41825}{339738624}\lambda^3 + \frac{1276387}{12230590464}\lambda^2 + \frac{692812541}{17978967982080}\lambda + \frac{18307106611}{3451961852559360}$